Multiple Aromaticity and Antiaromaticity in Silicon Clusters

Hua-Jin Zhai,[a] Aleksey E. Kuznetsov,[b] Alexander I. Boldyrev,*[b] and Lai-Sheng Wang*[a]

A series of silicon clusters containing four atoms but with different charge states (Si_4^{2+}, Si_4, Si_4^{2-}, and $NaSi_4^-$) were studied by photoelectron spectroscopy and ab initio calculations. Structure evolution and chemical bonding in this series were interpreted in terms of aromaticity and antiaromaticity, which allowed the prediction of how structures of the four-atom silicon clusters change upon addition or removal of two electrons. It is shown that Si_4^{2+} is square-planar, analogous to the recently discovered aromatic Al_4^{2-} cluster. Upon addition of two electrons, neutral Si_4 becomes σ-antiaromatic and exhibits a rhombus distortion. Adding two more electrons to Si_4 leads to two energetically close structures of Si_4^{2-}: either a double antiaromatic parallelogram structure or an aromatic system with a butterfly distortion. Because of the electronic instability of doubly charged Si_4^{2-}, a stabilizing cation (Na^+) was used to produce Si_4^{2-} in the gas phase in the form of $Na^+[Si_4^{2-}]$, which was characterized experimentally by photoelectron spectroscopy. Multiple antiaromaticity in the parallelogram $Na^+[Si_4^{2-}]$ species is highly unusual.

Introduction

Silicon is the backbone of the electronics industry.[1] The continued miniaturization of electronic devices is pushing towards the nano- and molecular scales. Hence, it is important to understand the physical and chemical properties of silicon clusters with a few to hundred of atoms. Indeed, silicon clusters have been the subject of extensive experimental and theoretical studies in the past two decades.[2–27] We have recently shown that the aromaticity and antiaromaticity concepts,[28] which are highly successful in organic chemistry, can be used to understand chemical bonding in all-metal clusters,[29–32] pnicogen clusters (Pn_5^- and Pn_4^{2-}; Pn = P, As, Sb),[33,34] and boron clusters (B_n^-, n = 3–15).[35–40] The Al_4^{2-} unit in bimetallic compounds MAl_4^- (M = Li, Na, Cu) was characterized as being aromatic with two delocalized π electrons. Thus, it follows the $4n+2$ Hückel rule for classical aromaticity.[29] This unit assumes a square-planar structure and maintains its structural and electronic integrity in the MAl_4^- complexes. The aromaticity of Al_4^{2-} was further investigated in several theoretical calculations.[41–43] By adding two more electrons to Al_4^{2-}, the Al_4^{4-} species was shown to be antiaromatic with four π electrons and a rectangular shape,[30] analogous to the structural distortion in cyclobutadiene, the quintessential antiaromatic organic compound, although the simultaneous presence of π antiaromaticity along with σ aromaticity in Al_4^{4-} has generated extensive discussions on its overall aromaticity or antiaromaticity.[30,44–47]

In our work on tetrapnicogens (Pn_4; Pn = P, As, Sb),[34] we showed how an extra electron distorted the tetrahedral Pn_4 and led to a roof-shaped ground state for Pn_4^-. Interestingly, the addition of a second electron completely flattened the tetramer and led to a square-planar ground state for Pn_4^{2-}. The Pn_4^{2-} species were produced in the gas phase in the form of $NaPn_4^-$ and were characterized by photoelectron spectroscopy and ab initio calculations as being aromatic with six π electrons.[34] Shortly after that, aromatic P_4^{2-} was synthesized in a bulk compound,[48] a demonstration that the concept of aromaticity is useful not only for the interpretation of novel molecular structures but also for "designing" novel materials. In our work on boron clusters, we observed and confirmed the presence of hepta- and octacoordinated boron species in molecular wheels of eight- and nine-atom boron clusters, and revealed, by molecular orbital analyses, that they possess double (π and σ) aromaticity, and that their molecular orbitals show "disk delocalization", which is responsible for the novel molecular structures and the extreme coordination environments.[38] For even larger boron clusters (with 10 to 15 atoms), we confirmed that they all prefer planar or quasiplanar structures, and showed that they exhibit aromaticity and antiaromaticity according to the Hückel rules, akin to planar hydrocarbons.[39] Small carborane molecules that contain three- and four-membered rings have been synthesized and shown to exhibit both σ and π aromaticity.[49–53]

Herein, we report the experimental and theoretical characterization of aromaticity and antiaromaticity in a series of silicon clusters that contain four atoms but with different charge states. We show that Si_4^{2+} is square-planar, analogous to the

[a] *Dr. H.-J. Zhai, Prof. Dr. L.-S. Wang*
Department of Physics, Washington State University
2710 University Drive, Richland, WA 99352 (USA) and
W. R. Wiley Environmental Molecular Sciences Laboratory
Pacific Northwest National Laboratory
MS K8-88, P. O. Box 999, Richland, WA 99352 (USA)
Fax: (+1) 509–376–6066
E-mail: ls.wang@pnl.gov

[b] *Dr. A. E. Kuznetsov, Prof. Dr. A. I. Boldyrev*
Department of Chemistry and Biochemistry
Utah State University, Logan, UT 84322 (USA)
E-mail: boldyrev@cc.usu.edu

Supporting information for this article is available on the WWW under http://www.chemphyschem.org or from the author.

 DOI: 10.1002/cphc.200400077

recently discovered aromatic Al_4^{2-} cluster. Upon addition of two electrons, the neutral Si_4 becomes σ-antiaromatic and exhibits a rhombus distortion. Adding two electrons to Si_4 leads either to a double antiaromatic Si_4^{2-} cluster, with a parallelogram structure, or to an aromatic system with a butterfly distortion. These two structures are close in energy and were observed experimentally in $Na^+[Si_4^{2-}]$ by photoelectron spectroscopy. The Na^+ ion was used here to stabilize the electronically unstable Si_4^{2-} structure, similar to our previous strategy used for stabilizing aromatic Al_4^{2-} and antiaromatic Al_4^{4-}.[29,30] The multiply antiaromatic $NaSi_4^-$ parallelogram species is highly unusual.[40] The concepts of aromaticity and antiaromaticity enable us to predict how structures of the four-atom silicon clusters change upon addition or removal of two electrons. These chemical concepts may be useful in understanding the electronic structure and chemical bonding in larger silicon clusters and in designing silicon or other semiconductor nanostructures for miniature electronic devices.

Structure and Bonding in Si_4^{2+}, Si_4, Si_4^{2-}, and $NaSi_4^-$

The finite size of clusters dictates that their geometric and electronic structures depend on the number of atoms in the cluster and its charge state. Let us consider a series of four-atom silicon clusters, Si_4^{2+}, Si_4, and Si_4^{2-}, which differ by a pair of electrons. First we searched for the global minimum structure for each cluster using ab initio calculations. This search yielded a number of local minima. The ground states and a selected set of singlet isomers for each charge state are presented in Figure 1. All other isomers including both singlet and triplet states are given in Figure S1 and Table S1 (Supporting Information).

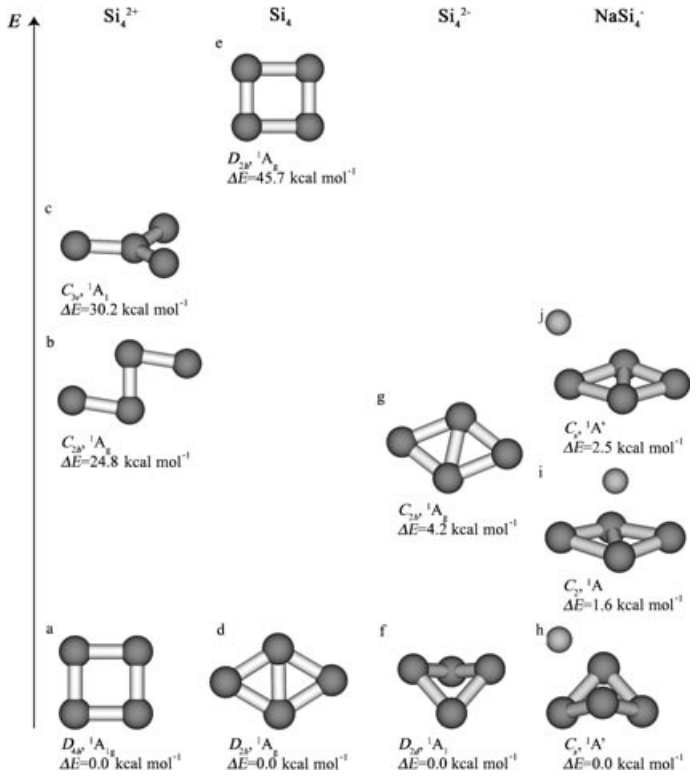

Figure 1. *Optimized structures of Si_4^{2+} (a–c), Si_4 (d, e), Si_4^{2-} (f, g), and $NaSi_4^-$ (h–j). The relative energies for all isomers are at the CCSD(T)/6-311+G(2df)//CCSD(T)/6-311+G* level of theory.*

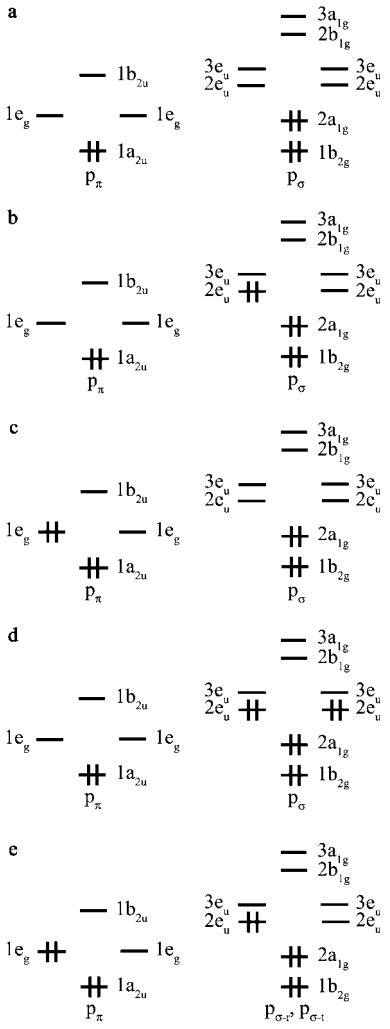

Figure 2. *Molecular orbital schemes for Si_4^{2+} (a), Si_4 (b, c), and Si_4^{2-} (d, e) D_{4h}, $^1A_{1g}$ species.*

The Si_4^{2+} dication is isoelectronic to the Al_4^{2-} dianion, which was shown previously to be a triply aromatic system (π-aromatic and doubly σ-aromatic).[29,41–43] The triple aromaticity in square-planar Al_4^{2-} comes from the three types of molecular orbitals (MOs) formed by the three 3p atomic orbitals (AOs) of Al (Figure 2): p_π (π orbitals perpendicular to the plane of the square from p_z AOs), $p_{\sigma\text{-}r}$ (σ orbitals oriented radially towards the center of the square from the $p_{x,y}$ AOs), and $p_{\sigma\text{-}t}$ (σ orbitals oriented tangentially around the square from the $p_{x,y}$ AOs). The lowest lying MO in each set is completely bonding, whereas the highest lying MO is completely antibonding. The two MOs in between are doubly degenerate with bonding/antibonding (or nonbonding) character. The

two types of $p_{\sigma\text{-}r}$ and $p_{\sigma\text{-}t}$ MOs are somewhat mixed and are presented as one set. On the basis of these three distinct types of MOs, we can introduce three types of aromaticity: π aromaticity from the p_π MOs, and two types of σ aromaticity from the $p_{\sigma\text{-}r}$ and $p_{\sigma\text{-}t}$ MOs. The occupation of all three bonding MOs in Al_4^{2-} makes it a perfect square and renders it triply aromatic. The bonding in Si_4^{2+} is identical to that in Al_4^{2-} (Figure 2a). It also has a perfectly square global minimum structure (Figure 1a), despite the fact that a zigzag structure (Figure 1b) offers better charge separation and should be favored electrostatically for a doubly charged cation.

When a pair of electrons is added to Si_4^{2+}, the resulting neutral Si_4 is expected to be either π-antiaromatic or σ_r-antiaromatic, depending on which MO the extra electrons occupy. The σ_r-antiaromatic system (Figure 2b) is expected to be rhombic, and the π-antiaromatic system (Figure 2c) is expected to be rectangular. The rhombus structure (Figure 1d) was found to be the global minimum, and the rectangular structure (Figure 1e) was found to be a second-order saddle point and substantially higher in energy. The rhombus structure, first predicted by Raghavachari and Logovinski,[15] is well known to be the global minimum for Si_4, and the σ_r-antiaromaticity of Si_4 provides the natural explanation for the rhombic distortion. However, the Si_4 rhombus can still be viewed as π-aromatic and σ_t-aromatic due to the presence of the two fully bonding π and σ_t MOs.

The most remarkable transformation occurs upon addition of an electron pair to neutral Si_4 to form the Si_4^{2-} dianion. Now we have several choices. We can add an electron pair to the σ_r-system of the σ_r-antiaromatic Si_4, thus completing the formation of four two-center, two-electron Si–Si bonds (Figure 2d). This Si_4^{2-} dianion should be considered as a classical 2π system and should be square-planar, but sp hybridization leads to a butterfly distortion (Figure 1f), which is analogous to the structural distortion in another classical π-aromatic system, namely, $C_4H_4^{2-}$.[54] The butterfly structure proved to be the global minimum for Si_4^{2-} according to our calculations. Alternatively, we can add a pair of electrons to the π system in the σ_r-antiaromatic rhombus Si_4 structure, which yields a doubly (σ_r- and π-) antiaromatic Si_4^{2-} structure (Figure 2e). Double antiaromaticity has an extremely interesting structural consequence. As mentioned above, σ_r antiaromaticity induces a rhombic distortion, and π-antiaromaticity a rectangular distortion. Hence, for a system with both σ_r- and π-antiaromaticity, one would expect a geometry that represents a compromise between the rhombic and rectangular distortions, that is, a parallelogram structure. Our calculations indeed yielded such a doubly antiaromatic structure (Figure 1g), which is 4.2 kcal mol^{-1} higher in energy than the global minimum butterfly structure.

The doubly charged and doubly antiaromatic Si_4^{2-} can exist only as a metastable species and cannot be studied experimentally as an isolated species. However, a counterion, such as Na^+, can stabilize it in the form of $NaSi_4^-$, which should be electronically and thermodynamically stable and can be studied in the gas phase by anionic photoelectron spectroscopy. In fact, the $NaSi_4^-$ anion has indeed been studied previously by photoelectron spectroscopy and ab initio calculations,[11] except that in the previous study no spectral features were resolved due to low spectral resolution.

An extensive search for the $NaSi_4^-$ global minimum was performed (alternative structures are given in Figure S2 and Table S2, Supporting Information). The most stable structure at the B3LYP/6–311+G* level of theory was found to be a rhombus (Figure 1j and Figure 3c), and a butterfly structure (Figure 1h and Figure 3a) and a parallelogram structure (Figure 1i and Figure 3b) are higher in energy by 1.1 and 3.5 kcal mol^{-1}, respectively. The lowest energy structures were recalculated including geometry optimization and frequency calculations at the CCSD(T)/6-311+G* level of theory. Finally, single-point calculations were performed for the same structures at the CCSD(T)/6-311+G(2df) level of theory. At the CCSD(T)/6-311G(2df) level of theory, the order of these structures was found to be different. The structure in which Na^+ is coordinated to the butterfly form of Si_4^{2-} is the most stable at the CCSD(T)/6-311+G(2df) level of theory, and the parallelogram and rhombus structures are higher in energy by 1.6 and 2.5 kcal mol^{-1}, respectively (Figure 1). The last two structures originate from the parallelogram structure of Si_4^{2-} and differ in the position of Na^+. Because the relative stabilities for the three lowest $NaSi_4^-$ structures depend on the theoretical

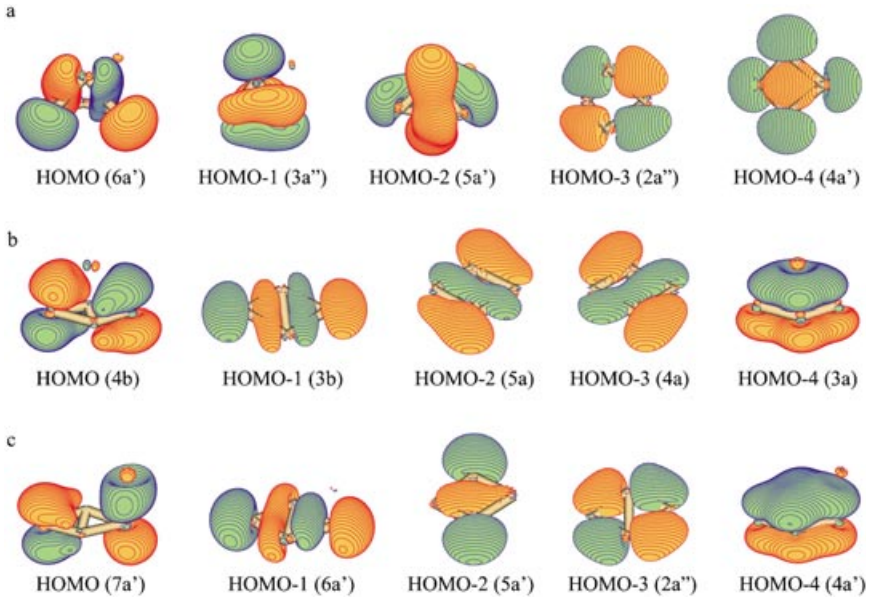

Figure 3. *Molecular orbital pictures for the three isomers of $NaSi_4^-$. a) Butterfly structure. b) Parallelogram structure. c) Rhombus structure.*

Table 1. *Experimental and theoretical vertical electron detachment energies [eV] for three $NaSi_4^-$ isomers.*

Band	VDE (exptl)	C_s, $^1A'$, "rhombus"				C_s, $^1A'$, "butterfly"				C_2, ^1A, "parallelogram"			
		MO	VDE ROVGF[a]	VDE TD B3LYP[b]	VDE TD BPW91[c]	MO	VDE ROVGF[a]	VDE TD B3LYP[b]	VDE TD BPW91[c]	MO	VDE ROVGF[a]	VDE TD B3LYP[b]	VDE TD BPW91[c]
X	1.52(3)	7a′	1.39 (0.85) [1.45]	1.59	1.58					4b	1.54 (0.88) [1.61]	1.55	1.56
a	1.8–2.4					6a′	1.93 (0.87) [2.00]	2.01	1.97				
						3a″	2.07 (0.87)	2.15	2.09				
A	2.74(2)	6a′	2.73 (0.84)	2.80	2.73					3b	2.57 (0.86)	2.65	2.57
b	≈3.0					5a′	2.94 (0.87)	2.98	3.01	5a	3.00 (0.86)	2.99	2.94
						2a″	3.00 (0.87)	2.99	2.96				
B	3.34(2)	5a′	3.24 (0.85)	3.28	3.11	4a′	3.39 (0.86)	3.40	3.38				
		2a″	3.31 (0.84)	3.39	3.40								
C	3.63(4)									4a	3.61 (0.86)	3.54	3.53
		4a′	4.14 (−0.19)	3.81	3.79					3a	3.99 (1.00)	3.89	3.91

[a] The VDEs were calculated at the ROVGF/6–311+G(2df)//CCSD(T)/6–311+G* level of theory. The numbers in the parentheses indicate the pole strength, which characterizes the validity of the one-electron detachment picture. The VDEs evaluated at the CCSD(T)/6–311+G(2df)/CCSD(T)/6–311+G* level of theory are given in brackets. [b] The VDEs were calculated at the TD B3LYP/6–311+G(2df)//CCSD(T)/6–311+G* level of theory. [c] The VDEs were calculated at the TD BPW91/6–311+G(2df)//CCSD(T)/6–311+G* level of theory.

method and because they are all very close to each other in energy, we cannot solely rely on the computational predictions. Instead, we obtained additional insight from comparisons between the experimental photoelectron spectrum and detachment energies calculated for the three lowest-lying structures (Table 1).

Photoelectron Spectra of $NaSi_4^-$

The photoelectron spectra of $NaSi_4^-$ are shown in Figure 4 at three photon energies.[55,56] Three sharp and intense bands (X, A, B) and two broad and weak bands (a and b) were resolved at 355 nm (Figure 4a). The peak maximum of band X defined the ground state vertical detachment energy (VDE) of 1.52 eV. Since no vibrational structures were resolved, the electron affinity of $NaSi_4$ was evaluated from the well-defined onset of band X by drawing a straight line at the leading edge of the band and then adding the instrumental resolution to the intersection with the binding-energy axis. The electron affinity thus evaluated is 1.49 ± 0.04 eV. Bands A at 2.74 eV and B at 3.34 eV were similarly sharp to band X, whereas bands a and b were broad. Band a covered a binding energy range of 1.8–2.4 eV, which appeared to contain two partially resolved features. Band b was largely buried between the two strong bands A and B. One more band C was observed at about 3.6 eV in the 266 nm spectrum (Figure 3b), with much weaker intensity than bands X, A, and B. No prominent transitions were observed beyond 4.0 eV at 193 nm (Figure 3c).

The complicated photoelectron spectral patterns and the presence of relatively weak features suggested that multiple isomers might exist in the cluster beam. The PES spectra implied that at least two isomers were likely present in the cluster beam: bands X, A, B, and possibly C came from the main isomer, and the weak and broad bands a and b from a weakly populated isomer.

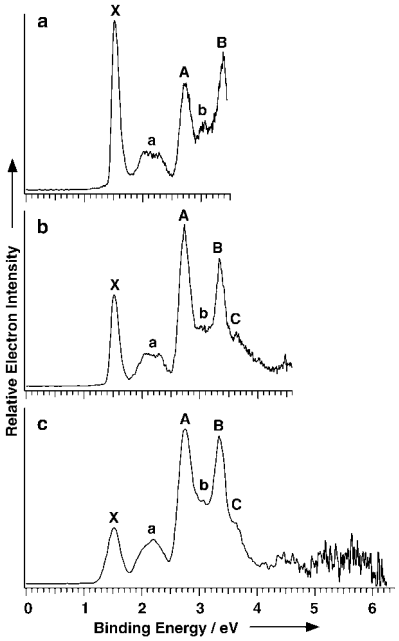

Figure 4. *Photoelectron spectra of $NaSi_4^-$ at a) 355 nm (3.496 eV), b) 266 nm (4.661 eV), and c) 193 nm (6.424 eV). The vertical detachment energies for the four major detachment features (X, A, B, C) are given in Table 1.*

Interpretation of the Photoelectron Spectra

The possible existence of multiple isomers, indicated in the PES data, is in qualitative agreement with the theoretical findings. To interpret the experimental data quantitatively, VDEs were calculated for the three low-lying isomers of $NaSi_4^-$. The theoretical photoelectron spectra, calculated at four different levels of theory, agree well with each other (Table 1) and lend considerable confidence to the theoretical predictions. The rhombus (Figure 1j) and parallelogram (Figure 1i) $NaSi_4^-$ are

different in energy by only 0.9 kcal mol^{-1} and differ simply by the position of the Na^+ cation. They give very similar VDEs and should contribute to the same detachment features. Thus the threshold peak X should correspond to electron detachment from the π-antibonding HOMO of the rhombus (7a′, Figure 3c) and parallelogram (4b, Figure 3b) structures, and the low detachment energy (1.52 eV) is consistent with the antibonding nature of these MOs. The calculated first VDE for the rhombus and the parallelogram isomers at all levels of theory agree well with the experimental value (Table 1).

The broad and weak features between 1.8 and 2.4 eV do not correspond to any one-electron processes from the rhombus or parallelogram structures, but agree very well with the two lowest transitions from the butterfly isomer of $NaSi_4^-$ (Table 1). The next prominent feature, A at 2.74 eV, is in excellent agreement with the second VDE (2.73 eV) calculated for the rhombus structure and in good agreement with the second VDE (2.57 eV) for the parallelogram structure. Again, the weak features around 3.0 eV in the experimental spectra can be assigned to the butterfly isomer, which has two transitions at 2.94 and 3.00 eV. The prominent feature B at 3.34 eV is in good agreement with the third and fourth detachment channels of the $NaSi_4^-$ rhombus structure, but may also contain contributions from the fifth detachment channel of the butterfly isomer (Table 1). Feature C at 3.63 eV is assigned to the fourth one-electron transition from the parallelogram isomer. The calculated VDEs for the higher energy detachment channels became unreliable, as shown by the poor pole strengths in ROVGF calculations (Table 1). Overall, the calculated spectra for the three isomers of $NaSi_4^-$ are in excellent agreement with the observed photoelectron spectra, and show convincingly that all three isomers contribute to the experimental spectra.

Discussion

The Si_4 cluster has been extensively studied both experimentally and theoretically.[2–4,7,9–11,14–22,25–27] Raman spectra[7] and IR absorption[9,10] spectra were recorded for neutral Si_4. Recently, Si_4 clusters were also prepared on an inert surface.[14] Photoelectron spectra,[2–4,13] as well as electronic absorption spectra,[10] of Si_4^- have been reported. A photoelectron spectrum was also reported previously for $NaSi_4^-$ at 355 nm,[11] but no spectral features were resolved due to low spectral resolution. Theoretically, the rhombus structure (Figure 1d) for Si_4 was established first by Raghavachari and Logovinski[15] and confirmed by numerous other calculations.[7,9,14–16,19–22,26,27] A similar structure was also obtained for the Si_4^- anion.[17,18,25] Theoretical calculations have also been performed for $NaSi_4^-$, and both parallelogram-based structures (Figure 1i and j) were identified.[11] However, the butterfly structure for $NaSi_4^-$ (Figure 1h) was not considered before, and the existence of multiple isomers has not been confirmed experimentally.

Our analysis of chemical bonding in this series of species clearly demonstrated how chemical bonding dictates the structures, and how the structures evolve from $Si_4^{2+} \rightarrow Si_4 \rightarrow Si_4^{2-} \rightarrow NaSi_4^-$. The structure and bonding in this series of species can be interpreted and understood by using the concept of multiple aromaticity and antiaromaticity. All three predicted low-lying isomers of $NaSi_4^-$ were produced experimentally and characterized by photoelectron spectroscopy (Figure 4). The parallelogram distortion of $NaSi_4^-$ clearly shows how both σ and π antiaromaticity distort aromatic and square-planar Si_4^{2+} by sequential addition of two pairs of electrons, with the rhombus Si_4 (π-aromatic and σ-antiaromatic) as an interim species. The parallelogram isomers of $NaSi_4^-$ are highly unusual species, and are among the very few doubly σ- and π-antiaromatic chemical species identified heretofore.[40]

Chemical Bonding in Four-Atom Cyclic Species of Main Group Elements

The current work also has some general implications for understanding the chemical bonding of cyclic tetramers from main group elements. Let us consider the planar square structure of Ar_4 as a model system. Figure 5 shows all MOs generated by

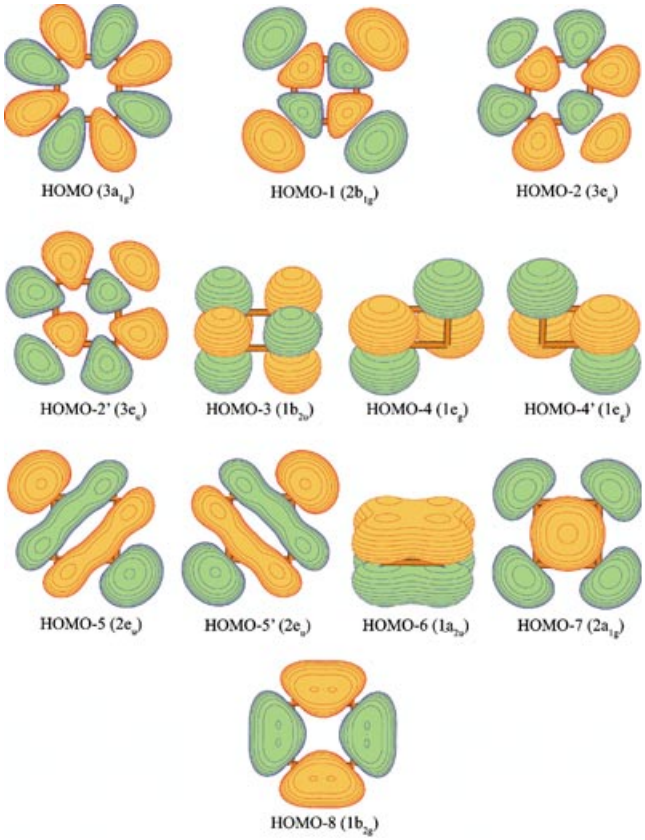

Figure 5. *Molecular orbitals for square-planar Ar_4 (D_{4h}, $^1A_{1g}$).*

p_π, $p_{\sigma\text{-}n}$, and $p_{\sigma\text{-}t}$ AOs of the Ar atoms. We can clearly identify three sets of MOs: p_π-based (HOMO-6, HOMO-4′, HOMO-4, HOMO-3), $p_{\sigma\text{-}r}$-based (HOMO-7, HOMO-2′, HOMO-2, HOMO-1), and $p_{\sigma\text{-}t}$-based (HOMO-8, HOMO-5′, HOMO-5, HOMO). For each set of MOs, the lowest energy one is completely bonding, the highest lying one is completely antibonding, whereas the two in between are doubly degenerate with bonding/antibonding (or nonbonding) character. The MOs for any sp four-atom

cyclic system are basically similar to those in Ar_4, except that the orders may vary and the occupation of the MOs depends on the number of valence electrons available.

For Al_4^{2-} and Si_4^{2+} (Figure 1), which are valence isoelectronic, only six p electrons are available, and all three bonding p MOs ($1b_{2g}$, $2a_{1g}$, and $1a_{2u}$) are occupied, resulting in two highly aromatic systems (π-aromatic and doubly σ-aromatic).[29,41–43] For Al_4^{4-}, the two extra electrons enter a π MO (similar to $1e_g$ in Figure 5), which leads to a 4π antiaromatic system with a rectangular structural distortion.[30] However, this system remains aromatic in the σ framework due to the occupation of two delocalized σ-bonding MOs. In Si_4, the two extra electrons enter the σ_r MO, which leads to a σ-antiaromatic system with a rhombus distortion (Figure 1), but Si_4 retains π aromaticity due to the two delocalized π electrons. In forming Si_4^{2-}, the two extra electrons could enter the σ_r or π MO of Si_4. The former remains π-aromatic but is subject to a butterfly distortion (Figure 1), while the latter is both π- and σ-antiaromatic and distorts to a unique parallelogram shape (Figure 1), an exact compromise between the rectangular distortion of π antiaromaticity and the rhombus distortion of σ antiaromaticity.

Consider another example, P_4^{2-}. It has fourteen valence electrons, and six of these enter three π MOs (similar to $1a_{2u}$ and $1e_g$ in Figure 5), which completely flattened the tetrahedral P_4 neutral and led to a 6π aromatic system with a perfectly planar square shape.[34] Aromatic P_4^{2-} was recently synthesized in a bulk compound.[48] Finally, for Ar_4, all bonding, nonbonding, and antibonding MOs based on p_π, $p_{\sigma\text{-}n}$ and $p_{\sigma\text{-}t}$ AO_s are occupied, and all MOs listed in Figure 5 add up to twelve lone pairs and result in no net bonding in Ar_4, which is a weakly bound van der Waals cluster.

Conclusions

We have reported the experimental and theoretical characterization of aromaticity and antiaromaticity in a series of silicon clusters containing four atoms but with different charge states. We showed that Si_4^{2+} is square-planar, analogous to the recently discovered aromatic Al_4^{2-} cluster. Upon addition of two electrons, neutral Si_4 becomes σ-antiaromatic, which results in a rhombic distortion. Adding two electrons to Si_4 leads to either a double antiaromatic Si_4^{2-} system with a parallelogram structure, or to an aromatic system with a butterfly distortion. These two structures are close in energy and were observed experimentally in $NaSi_4^-$ by photoelectron spectroscopy. We have demonstrated how the molecular orbital analyses and the concepts of π and σ aromaticity and antiaromaticity can be used to relate and understand the structure and chemical bonding of a series of four-silicon clusters in different charge states. Similar analyses and results should hold for other semiconductor clusters, such as Ge_4 or Ga_2As_2. It is believed that such an approach may be highly profitable in understanding and elucidating the structures and bonding in other small semiconductor clusters and how they evolve with charging and discharging. The changes in cluster structures induced by charging may be a valuable concept for assessing the suitability of a given nanocluster for potential device applications.

Experimental Section

Photoelectron Spectroscopy: Details of the photoelectron spectroscopy apparatus have been described elsewhere.[55,56] The sodium–silicon mixed cluster anions were generated by laser vaporization of a Na/Si disk target (30 mol% Na) in the presence of helium carrier gas and analyzed by time-of-flight mass spectrometry. The $NaSi_4^-$ anion was mass-selected and decelerated before being photodetached by a pulsed laser beam. Photoelectrons were collected at nearly 100% efficiency by a magnetic bottle and analyzed in a 3.5 m long electron flight tube. The PES spectra were calibrated by using the known spectrum of Rh^-, and the energy resolution was $\Delta Ek/Ek \approx 2.5\%$, that is, approximately 25 meV for 1 eV electrons.

Theoretical Methods: The initial search for the most-stable structures was performed with a hybrid method, which is known in the literature as B3LYP,[57–59] with the polarized split-valence basis sets (6-311+G*).[60,61] The lowest few structures in every system were then refined by the coupled-cluster method with single, double, and noniterative triple excitations [CCSD(T)][62,63] with the same basis sets. Total energies of these structures were also calculated with the extended 6-311+G(2df) basis sets. The vertical electron detachment energies (VDEs) were calculated using CCSD(T)/6-311+G(2df) and the outer valence Green Function method [OVGF/6-311+G(2df)].[64–68] VDEs were also calculated by the time-dependent DFT method [TD B3LYP/6-311+G(2df) and TD BPW91/6-311+G(2df)].[69, 70] In this approach, VDEs were calculated as a sum of the lowest transitions from the singlet anion into the lowest doublet state of the neutral species (at the B3LYP or BPW91 level of theory), and the vertical excitation energies in the neutral species (at the TD-B3LYP or TD-BPW91 level of theory, respectively). Core electrons were frozen in treating the electron correlation at the CCSD(T) and OVGF levels of theory. All calculations were performed with Gaussian 98[71] and Gauusian 03[72] programs on a 63-node Birch–Retford Beowulf cluster computer built at Utah State University by K. A. Birch and B. P. Retford. Molecular orbital pictures (RHF/6-311+G*) were made by using the MOLDEN 3.4 program.[73]

Acknowledgements

Theoretical work at Utah was supported by the donors of the Petroleum Research Fund (PRF#38242-AC6), administrated by the American Chemical Society. Experimental work at Washington was supported by the National Science Foundation (DMR-0095828 to L.S.W.) and performed at the W. R. Wiley Environmental Molecular Science Laboratory, a national scientific user facility sponsored by the Office of Biological and Environmental Research of the U.S. Department of Energy (DOE) and located at the Pacific Northwest National Laboratory, which is operated for DOE by Battelle.

Keywords: antiaromaticity · aromaticity · cluster compounds · photoelectron spectroscopy · silicon

[1] D. A. B. Miller, *Nature* **1996**, *384*, 307.
[2] O. Cheshnovsky, S. H. Yang, C. L. Pettiette, M. J. Craycraft, Y. Liu, R. E. Smalley, *Chem. Phys. Lett.* **1987**, *138*, 119.
[3] T. N. Kitsopoulos, C. J. Chick, A. Weaver, D. M. Neumark, *J. Chem. Phys.* **1990**, *93*, 6108.
[4] C. Xu, T. R. Taylor, G. R. Burton, D. M. Neumark, *J. Chem. Phys.* **1998**, *108*, 1395.
[5] M. F. Jarrold, *Science* **1991**, *252*, 1085.

[6] M. F. Jarrold, V. A. Constant, *Phys. Rev. Lett.* **1991**, *67*, 2994.
[7] E. C. Honea, A. Ogura, C. A. Murray, K. Raghavachari, W. O. Sprenger, M. F. Jarrold, W. L. Brown, *Nature* **1993**, *366*, 42.
[8] K.-H. Ho, A. A. Shvartsburg, B. Pan, Z.-Y. Lu, C.-Z. Wang, J. G. Wacker, J. L. Fye, M. F. Jarrold, *Nature* **1998**, *392*, 582.
[9] S. Li, R. J. Van Zee, W. Weltner, Jr., K. Raghavachari, *Chem. Phys. Lett.* **1995**, *243*, 275.
[10] J. Fulara, P. Freivogel, M. Grutter, J. P. Maier, *J. Phys. Chem.* **1996**, *100*, 18042.
[11] R. Kishi, H. Kawamata, Y. Negishi, S. Iwata, A. Nakajima, K. Kaya, *J. Chem. Phys.* **1997**, *107*, 10029.
[12] J. Muller, B. Liu, A. A. Shvartsburg, S. Ogut, J. R. Chelokowsky, K. W. Michael Siu, K. M. Ho, G. Gantefor, *Phys. Rev. Lett.* **2000**, *85*, 1666.
[13] M. A. Hoffman, G. Wrigge, B. v. Issendorff, J. Muller, G. Gantefor, H. Haberland, *Eur. Phys. J. D* **2001**, *16*, 9.
[14] M. Grass, D. Fischer, M. Mathes, G. Gantefor, P. Nielaba, *Appl. Phys. Lett.* **2002**, *81*, 3810.
[15] K. Raghavachari, V. Logovinsky, *Phys. Rev. Lett.* **1985**, *55*, 2853.
[16] K. Raghavachari, *J. Chem. Phys.* **1986**, *84*, 5672.
[17] K. Raghavachari, C. M. Rohlfing, *J. Chem. Phys.* **1991**, *94*, 3670.
[18] C. M. Rohlfing, K. Raghavachari, *J. Chem. Phys.* **1992**, *96*, 2114.
[19] G. Pacchioni, J. Koutecky, *J. Chem. Phys.* **1986**, *84*, 3301.
[20] K. Balasubramanian, *Chem. Phys. Lett.* **1987**, *135*, 283.
[21] C. H. Patterson, R. P. Messmer, *Phys. Rev. B* **1990**, *42*, 7530.
[22] R. Fournier, S. B. Sinnott, A. E. DePristo, *J. Chem. Phys.* **1992**, *97*, 4149.
[23] D. J. Wales, *Phys. Rev. A*, **1994**, *49*, 2195.
[24] J. C. Grossman, L. Mitas, *Phys. Rev. Lett.* **1995**, *74*, 1323.
[25] N. Binggeli, J. R. Chelikowsky, *Phys. Rev. Lett.* **1995**, *75*, 493.
[26] J. A. Niesse, H. R. Mayne, *Chem. Phys. Lett.* **1996**, *261*, 576.
[27] S. Wei, R. N. Barnett, U. Landman, *Phys. Rev. B* **1997**, *55*, 7935.
[28] See, for example, a special issue on aromaticity: *Chem. Rev.* **2001**, *101*, 1115 – 1566.
[29] X. Li, A. E. Kuznetsov, H. F. Zhang, A. I. Boldyrev, L. S. Wang, *Science* **2001**, *291*, 859.
[30] A. E. Kuznetsov, K. A. Birch, A. I. Boldyrev, X. Li, H. J. Zhai, L. S. Wang, *Science* **2003**, *300*, 622.
[31] A. E. Kuznetsov, A. I. Boldyrev, X. Li, L. S. Wang, *J. Am. Chem. Soc.* **2001**, *123*, 8825.
[32] A. E. Kuznetsov, A. I. Boldyrev, H. J. Zhai, X. Li, L. S. Wang, *J. Am. Chem. Soc.* **2002**, *124*, 11791.
[33] H. J. Zhai, L. S. Wang, A. E. Kuznetsov, A. I. Boldyrev, *J. Phys. Chem. A* **2002**, *106*, 5600.
[34] A. E. Kuznetsov, H. J. Zhai, L. S. Wang, A. I. Boldyrev, *Inorg. Chem.* **2002**, *41*, 6062.
[35] H. J. Zhai, L. S. Wang, A. N. Alexandrova, A. I. Boldyrev, *J. Chem. Phys.* **2002**, *117*, 7917.
[36] A. N. Alexandrova, A. I. Boldyrev, H. J. Zhai, L. S. Wang, E. Steiner, P. W. Fowler, *J. Phys. Chem. A* **2003**, *107*, 1359.
[37] H. J. Zhai, L. S. Wang, A. N. Alexandrova, A. I. Boldyrev, V. G. Zakrzewski, *J. Phys. Chem. A* **2003**, *107*, 9319.
[38] H. J. Zhai, A. N. Alexandrova, K. A. Birch, A. I. Boldyrev, L. S. Wang, *Angew. Chem.* **2003**, *115*, 6186; *Angew. Chem. Int. Ed.* **2003**, *42*, 6004; .
[39] H. J. Zhai, B. Kiran, J. Li, L. S. Wang, *Nature Mater.* **2003**, *2*, 827.
[40] A. N. Alexandrova, A. I. Boldyrev, H. J. Zhai, L. S. Wang, *J. Phys. Chem. A* **2004**, *108*, 3509.
[41] P. W. Fowler, R. W. A. Havenith, E. Steiner, *Chem. Phys. Lett.* **2001**, *342*, 85.
[42] J. Juselius, M. Straka, D. Sundholm, *J. Phys. Chem. A* **2001**, *105*, 9939.
[43] C.-G. Zhan, F. Zheng, D. A. Dixon, *J. Am. Chem. Soc.* **2002**, *124*, 14795.
[44] Z. Chen, C. Corminboeuf, T. Heine, J. Bohman, P. v. R. Schleyer, *J. Am. Chem. Soc.* **2003**, *125*, 13930.
[45] R. W. A. Havenith, P. W. Fowler, E. Steiner, S. Shetty, D. Kanhere, S. Pal, *Phys. Chem. Chem. Phys.* **2004**, *6*, 285.
[46] S. Shetty, D. Kanhere, S. Pal, *J. Phys. Chem. A*, **2004**, *108*, 628.
[47] S. K. Ritter, *Chem. Eng. News*, **2003**, December 15, 23.
[48] F. Kraus, J. C. Aschenbrenner, N. Korber, *Angew. Chem.* **2003**, *115*, 4162; *Angew. Chem. Int. Ed.* **2003**, *42*, 4030; .
[49] C. Präsang, A. Mlodzianowska, Y. Sahin, M. Hofmann, G. Geiseler, W. Massa, A. Berndt, *Angew. Chem.* **2002**, *114*, 3529; *Angew. Chem. Int. Ed.* **2002**, *41*, 3380; .
[50] C. Präsang, M. Hofmann, G. Geiseler, W. Massa, A. Berndt, *Angew. Chem.* **2002**, *114*, 1597; *Angew. Chem. Int. Ed.* **2002**, *41*, 1526; .
[51] C. Präsang, A. Mlodzianowska, G. Geiseler, W. Massa, M. Hofmann, A. Berndt, *Pure Appl. Chem.* **2003**, *75*, 1175.
[52] P. Amseis, W. Mesbah, C. Präsang, M. Hofmann, G. Geiseler, W. Massa, A. Berndt, *Organometallics* **2003**, *22*, 1594.
[53] W. Mesbah, C. Präsang, M. Hofmann, G. Geiseler, W. Massa, A. Berndt, *Angew. Chem.* **2003**, *115*, 1758; *Angew. Chem. Int. Ed.* **2003**, *42*, 1717; .
[54] M. Balci, M. L. McKee, P. von R. Schleyer, *J. Phys. Chem. A* **2000**, *104*, 1246.
[55] L. S. Wang, H. S. Cheng, J. Fan, *J. Chem. Phys.* **1995**, *102*, 9480.
[56] L. S. Wang, H. Wu in *Advances in Metal and Semiconductor Clusters. IV. Cluster Materials* (Ed.: M. A. Duncan), JAI, Greenwich, CT, **1998**, pp. 299 – 343.
[57] R. G. Parr, W. Yang, *Density-Functional Theory of Atoms and Molecules*, Oxford University Press, Oxford, **1989**.
[58] A. D. Becke *J. Chem. Phys.* **1993**, *98*, 5648.
[59] J. P. Perdew, J. A. Chevary, S. H. Vosko, K. A. Jackson, M. R. Pederson, D. J. Singh, C. Fiolhais, *Phys. Rev. B* **1992**, *46*, 6671.
[60] A. D. McLean, G. S. Chandler, *J. Chem. Phys.* **1980**, *72*, 5639.
[61] T. Clark, J. Chandrasekhar, G. W. Spitznagel, P. von R. Schleyer, *J. Comput. Chem.* **1983**, *4*, 294.
[62] J. Cizek, *Adv. Chem. Phys.* **1969**, *14*, 35.
[63] K. Raghavachari, G. W. Trucks, J. A. Pople, M. Head-Gordon, *Chem. Phys. Lett.* **1989**, *157*, 479.
[64] L. S. Cederbaum, *J. Phys B*, **1975**, *8*, 290.
[65] W. von Niessen J. Shirmer, L. S. Cederbaum, *Comput. Phys. Rep.* **1984**, *1*, 57.
[66] V. G. Zakrzewski, J. V. Ortiz, *Int. J. Quant. Chem.*, **1995**, *53*, 583.
[67] a) J. V. Ortiz, *Int. J. Quant. Chem. Quant. Chem. Symp.* **1989**, *23*, 321; b) J. S. Lin, J. V. Ortiz, *Chem. Phys. Lett.* **1990**, *171*,197.
[68] V. G. Zakrzewski, J. V. Ortiz, J. A. Nichols, D. Heryadi, D. L. Yeager, J. T. Golab, *Int. J. Quant. Chem. Quant.* **1996**, *60*, 29.
[69] R. Bauernshmitt, R. Alrichs, *Chem. Phys. Lett.* **1996**, *256*, 454.
[70] M. E. Casida, C. Jamorski, K. C. Casida, D. R. Salahub, *J. Chem. Phys.* **1998**, *108*, 4439.
[71] Gaussian 98 (revision A.7), M. J. Frisch, G. M. Trucks, H. B. Schlegel, G. E. Scuseria, M. A. Robb, J. R. Cheeseman, V. G. Zakrzewski, J. A. Montgomery, R. E. Stratmann, J. C. Burant, S. Dapprich, J. M. Millam, A. D. Daniels, K. N. Kudin, M. C. Strain, O. Farkas, J. Tomasi, V. Barone, M. Cossi, R. Cammi, B. Mennucci, C. Pomelli, C. Adamo, S. Clifford, J. W. Ochterski, G. A. Petersson, P. Y. Ayala, Q. Cui, K. Morokuma, P. Salvador, J. J. Dannenberg, D. K. Malick, A. D. Rabuck, K. Raghavachari, J. B. Foresman, J. Cioslowski, J. V. Ortiz, A. G. Baboul, B. B. Stefanov, G. Liu, A. Liashenko, P. Piskorz, I. Komaromi, R. Gomperts, R. L. Martin, D. J. Fox, T. Keith, M. A. Al-Laham, C. Y. Peng, A. Nanayakkara, M. Challacombe, P. M. W. Gill, B. G. Johnson, W. Chen, M. W. Wong, J. L. Andres, M. Head-Gordon, E. S. Replogle, C. Gonzales, J. A. Pople, Gaussian, Inc., Pittsburgh PA, **1998**.
[72] Gaussian 03 (revision A.1), M. J. Frisch, G. M. Trucks, H. B. Schlegel, G. E. Scuseria, M. A. Robb, J. R. Cheeseman, J. A. Montgomery, T Vreven, K. N. Kudin, J. C. Burant, J. M. Millam, S. S. Iyengar, J. Tomasi, V. Barone, B. Mennucci, M. Cossi, G. Scalmani, N. Rega, G. A. Petersson, H. Nakatsuji, O. Kitao, H. Nakai, M. Klene, X. Li, J. E. Knox, H. P. Hratchian, J. B. Cross, C. Adamo, J. Jaramillo, R. Gomperts, R. E. Stratmann, O. Yazyev, A. J. Austin, R. Cammi, C. Pomelli, J. W. Ochterski, P. Y. Ayala, K. Morokuma, G. A. Voth, P. Salvador, J. J. Dannenberg, V. G. Zakrzewski, S. Dapprich, A. D. Daniels, M. C. Strain, O. Farkas, D. K. Malick, A. D. Rabuck, K. Raghavachari, J. B. Foresman, J. V. Ortiz, Q. Cui, A. G. Baboul, S. Clifford, J. Cioslowski, B. B. Stefanov, G. Liu, A. Liashenko, P. Piskorz, I. Komaromi, R. L. Martin, D. J. Fox, T. Keith, M. A. Al-Laham, C. Y. Peng, A. Nanayakkara, M. Challacombe, P. M. W. Gill, B. G. Johnson, W. Chen, M. W. Wang, C. Gonzales, J. A. Gaussian, Inc., Pittsburgh PA, **2003**.
[73] G. Schaftenaar, MOLDEN3.4, CAOS/CAMM Center, The Netherlands, **1998**.

Received: February 24, 2004
Revised: June 6, 2004

Early View Article
Published online on November 8, 2004

